

# Peptide mass fingerprinting as a tool to assess micromammal biodiversity in Pleistocene South Africa: The case of Klipdrift Shelter

Turid Hillestad Nel<sup>a,\*</sup>, Carli Peters<sup>b,1</sup>, Kristine Korzow Richter<sup>c,1</sup>,  
Christopher Henschilwood<sup>a,d</sup>, Karen van Niekerk<sup>a,e</sup>, Katerina Douka<sup>f,g,\*\*</sup>

<sup>a</sup> SFF Centre for Early Sapiens Behaviour (SapienCE), University of Bergen, Post Box 7805, 5020, Bergen, Norway

<sup>b</sup> Department of Archaeology, Max Planck Institute of Geoanthropology, Jena, Germany

<sup>c</sup> Department of Anthropology, Harvard University, Boston, USA

<sup>d</sup> Evolutionary Studies Institute, University of the Witwatersrand, Johannesburg, South Africa

<sup>e</sup> School of Geography, Archaeology and Environmental Studies, University of Witwatersrand, Johannesburg, South Africa

<sup>f</sup> Department of Evolutionary Anthropology, Faculty of Life Sciences, University of Vienna, Austria

<sup>g</sup> Human Evolution and Archaeological Sciences (HEAS) Network, University of Vienna, Austria

## ARTICLE INFO

Handling Editor: Danielle Schreve

### Keywords:

Zooarchaeology by mass spectrometry (ZooMS)

Micromammals

Rodents

Middle stone age

South Africa

## ABSTRACT

Remains of small mammals from archaeological sites are often used as palaeoenvironmental proxies in the reconstruction of past environments. Yet, identification of micromammals to species-level based on morphological traits is often difficult due to fragmentation of diagnostic skeletal elements. Here we test the potential of Zooarchaeology by Mass Spectrometry (ZooMS) as a tool for the taxonomic identification of micromammal remains from Middle Stone Age (MSA) sequences in South Africa. ZooMS peptide markers are first established for 14 extant micromammal species present in the region. These novel peptide markers are then used to identify micromammal bone remains from the MSA levels of Klipdrift Shelter (c. 72–51 ka), De Hoop Nature Reserve, South Africa. Our study shows that collagen preservation in micromammal bones from MSA contexts is sufficient for successful ZooMS analysis. To our knowledge, these results represent the oldest material successfully analysed with ZooMS from an African context. The peptide markers developed as part of this study can be used to characterize a larger number of micromammal assemblages. This holds significant promise for the future application of ZooMS to prehistoric material in South Africa and elsewhere in the continent.

## 1. Introduction

### 1.1. Background

An essential question in human evolution studies is the role of climatic and vegetation changes as potential catalysts for human adaptability, changing mobility patterns and increased cultural complexity; developments that are frequently seen as main drivers for the widespread and often rapid dispersals of early hominins across Africa and Eurasia. In southern Africa, the Middle Stone Age archaeological record (MSA; 280,000–50/25,000 years ago (ka), [McBrearty and Brooks, 2000](#)) displays distinct variations in technological and cultural mechanisms and shifts in ecological niches, particularly between 100 and 50 ka

([d'Errico et al., 2017](#)). These changes are traditionally linked to increased human adaptation to an ever-changing environmental and climatic backdrop ([Mackay et al., 2014](#); [d'Errico et al., 2017](#); [Marean et al., 2020](#); [Mackay et al., 2022](#)).

Detailed reconstruction of environmental conditions directly experienced by these early humans is crucial for understanding resource procurement strategies, technological and cultural innovations, and site choices in the MSA. Analyses of micromammals incorporated into archaeological sediments can provide such direct information of past local environmental conditions (e.g. [Avery, 1979](#); [Avery, 1981](#); [Andrews, 1990](#); [Avery, 2002](#); [Matthews, 2004](#); [Matthews et al., 2009](#); [Matthews et al., 2011](#); [Stoetzel et al., 2011](#); [Stoetzel et al., 2018](#)). Micromammals, defined here as rodents, shrews and bats with a live

\* Corresponding author.

\*\* Corresponding author. Department of Evolutionary Anthropology, Faculty of Life Sciences, University of Vienna, Austria.

E-mail addresses: [Turid.Nel@uib.no](mailto:Turid.Nel@uib.no) (T.H. Nel), [katerina.douka@univie.ac.at](mailto:katerina.douka@univie.ac.at) (K. Douka).

<sup>1</sup> Equal contribution.

weight of <200 g, are particularly suitable palaeoenvironmental informants as they have small home-ranges (usually less than 1 km radius), many taxa have distinct ecological requirements, and they often respond to environmental changes within local spatiotemporal scales by population increase or rapid turnover (Korpimäki et al., 2004; Heisler et al., 2016; Reed et al., 2019). In Europe, East Africa, and South Africa, analyses of modern micromammals have demonstrated a close correlation between the relative abundance of species and the composition of vegetation substrate near sample sites (Andrews, 1990; Avery, 1992; Avery et al., 2005; Reed et al., 2019). Hence, collection and analyses of micromammal material from archaeological sites and sediments linked to human occupation offer a tremendous opportunity to understand local environmental conditions and variations therein through time, as well as highlighting human preferences and responses to environmental change over time.

Micromammals generally end up in archaeological deposits when predators (e.g. birds of prey and/or mammalian carnivores) deposit them in a site as prey (Andrews, 1990). In South African archaeological contexts, various species of owls have used rock shelters and caves as roosting sites intermittently with human occupation (Matthews, 2004; Matthews et al., 2005, 2009, 2011, 2020; Nel, 2013; Nel and Henshilwood, 2016, 2021; Nel et al., 2018). Owls cannot digest the fur and bones of their prey and regurgitate these remains as pellets, which end up on the floor of the cave/shelter. These remains then disintegrate and become part of archaeological deposits. Micromammal assemblages often contain a diverse range of taxa that can be difficult to distinguish by using morphological traits. Diagnostic features, and in particular dental elements, that are crucial to taxonomically identify micromammals, are often missing due to breakage, digestion, and other post-depositional processes. Additionally, many birds of prey remove the heads from their rodent prey prior to consuming the remainder of the carcass (e.g. Glue, 1967), leading to an absence of identifiable cranial material altogether. At the same time, morphological identification of micromammals based on postcranial remains is often not possible due to frequent fragmentation and osteological similarities between species. Increasing identification rates of micromammals from archaeological deposits would increase the potential of micromammals for reconstructing local environmental conditions, which in turn can inform us of the environments humans inhabited in the past.

Another major challenge when trying to reconstruct Pleistocene environments and understand human-animal and human-environment interactions in Africa is the assumed lack of biomolecular preservation. Ancient DNA (aDNA) preservation is often too poor and it has been proven extremely difficult to recover endogenous aDNA from contexts beyond the Later Stone Age (LSA, ~20 ka, e.g. Lipson et al., 2022). Ancient proteins are more resistant to harsh conditions, such as warm environments, compared to aDNA (Buckley et al., 2009), and also persist over longer periods of time (Demarchi et al., 2016, 2022). Palaeoproteomics thus offers an alternative route for investigating both the faunal and the hominin record in Africa and beyond, in a similar way that such methods have started being used in Pleistocene-age sites from other parts of the world, for example in Southeast Asia (Welker et al., 2019), where biomolecular preservation is equally challenging.

Here, we use Zooarchaeology by Mass Spectrometry (ZooMS), or peptide mass fingerprinting, a collagen-based taxonomic identification method, to overcome issues of fragmentation and preservation to identify morphologically undiagnostic micromammal bones. ZooMS can supplement and, in some cases, refine traditional zooarchaeological datasets, and provide valuable insights into palaeoenvironmental reconstructions and (micro)mammal community changes. The method is increasingly used to identify and characterize large mammalian assemblages from archaeological sites (e.g. Welker et al., 2015; Welker et al., 2016; Buckley et al., 2017; Welker et al., 2017; Sinet-Mathiot et al., 2019; Brown et al., 2021b; Silvestrini et al., 2022; Ruebens et al., 2023), but remains relatively unexplored for micromammals. ZooMS has been applied previously to identify murine rodents (Buckley et al.,

2016), arvicoline rodents (Buckley et al., 2018) and bats (Buckley and Herman, 2019) at the Late Pleistocene site of Pin Hole Cave, Creswell Crags (UK), demonstrating that some taxa can be distinguished to genus and in some cases species level. Peptide mass fingerprinting has also been used to track the introduction of non-native rodents to the coast of eastern Africa (Prendergast et al., 2017) and the Cayman Brac (Cayman Islands) (Harvey et al., 2019). In South Africa, ZooMS has been used previously to confirm the identification of the earliest domesticated sheep in the region at c. 2000 BP (Coutu et al., 2021), to provide insights into ivory trade between the 7th –10th centuries AD (Coutu et al., 2016), and to identify animal species that were used to manufacture bone tools from the 4th and 7th century AD (Bradfield et al., 2019) and from the first millennium AD contact period in the KwaZulu-Natal Province (Bradfield et al., 2021). Our feasibility study represents the first use of ZooMS to analyse MSA material from South Africa and is also the first systematic application of ZooMS on micromammal material from this part of the world. Additionally, to resolve unique peptide markers, peptide sequences was performed and we provide here new ZooMS peptide markers for 14 African micromammal species. We demonstrate the utility of these markers in the identification of micromammal bones from the MSA site of Klipdrift Shelter.

## 1.2. Sites

### 1.2.1. Archaeological site

Klipdrift Shelter (KDS) (34°27.09630 S, 20°43.45820 E) is situated in De Hoop Nature Reserve on the southern Cape coast, approximately 150 km southeast of Cape Town, South Africa (Henshilwood et al., 2014) at an elevation of c. 19 m above sea level (Fig. 1a). The shelter forms part of a larger cliff-face complex consisting of multiple truncated archaeological sites. The larger, western cave is c. 21 m deep and contains at least two sites, Klipdrift Cave (KDC) and Klipdrift Cave Lower (KDCL). KDC contains LSA deposits, and further dating efforts are required at KDCL to establish its chronology. KDS is separated from KDC and KDCL by a quartzite promontory and is c. 7 m deep. KDS contains MSA deposits and was first excavated in 2011 with subsequent seasons in 2012, 2013 and 2018. The MSA sequence at KDS has been dated to between c. 71.6 ± 5.1 ka (Layer PE) and 51.7 ± 3.3 ka (Layer PAN/PAO) by single grain Optically Stimulated Luminescence (OSL) methods (Henshilwood et al., 2014) (Fig. 1b). The Howiesons Poort (HP) sequence (PCA to PAY) at KDS is dated between 65.5 ± 4.8 ka and 59.4 ± 4.6 ka (Henshilwood et al., 2014).

### 1.2.2. Modern collection sites

Modern micromammal material to use as reference material for ZooMS was collected from seven modern owl roosting sites. Six of these sites are located in the De Hoop Nature Reserve, within a 32 km radius of KDS (Fig. 1a). Elandspad Farmhouse (34°25.198 S, 20°43.133 E) is an abandoned farmhouse, formerly recorded as a roosting site for owls and now seemingly deserted. Buffelsfontein Bush Camp Kraal (34°24.427 S, 20°35.284 E) is an open structure for farm animals, while De Mond (34°2.255 S, 20°25.456 E) is an abandoned farmstead. Both locations seemed to be transient places for roosting, and are possibly still in use. Three outhouses: Potberg Garage (34°22.310 S, 20°31.594 E), De Hoop Collections Cool Room (34°27.185, 20°23.530 E), and Melkkamer Barn (34°27.342 S, 20°23.255 E) were all still active barn owl (*Tyto alba*) roosting sites in October 2018, as barn owls were visually observed fleeing the outhouses when owl pellets were collected. The last modern collection site is Witels Farm (33°59.943 S, 21°32.394 E), c. 90 km northeast and inland from KDS, in the foothills of the Langeberg Mountains. It is an active barn owl roosting site in an abandoned house (Johan van Rooyen pers. comm. 05.04.19).



**Fig. 1a.** Map with the location of archaeological sites and modern owl pellet collection sites. BBC: Blombos Cave. BFB: Buffelsfontein Bush Camp Kraal. DHCC: De Hoop Collections Cool Room. DMB: De Mond. EPD: Elandspad Farmhouse. KDS: Klipdrift Shelter. MKB: Melkkamer Barn. PTB: Potberg Garage. WIT: Witels Farm. **1b:** Overview of the Klipdrift locality. Image courtesy of Magnus M. Haaland.

## 2. Material and methods

### 2.1. Materials

#### 2.1.1. Modern references

There are several excellent comparative collections of micromammal species housed at museums in South Africa which could contain suitable morphologically identified specimens that could have been used to develop a reference dataset. However, many museum specimens are chemically treated for conservation purposes, making them unsuitable for ZooMS analysis. We therefore used micromammal specimens manually separated from owl pellets. Unpublished analyses of the digestive tracts on micromammal incisors and molars from the MSA deposits at KDS establish the spotted eagle owl (*Bubo africanus*) as the main accumulator at KDS (Nel, unpublished data). Barn owls (accumulators of the modern pellets used in this study) and spotted eagle owls are opportunistic and hunt a similar range of micromammal taxa on the south coast of South Africa, with a preference for Otomyinae,

Gerbillinae, and Soricids (Avery et al., 2005; Matthews et al., 2011, 2020). The co-occurrence of these two predators at archaeological sites is known from Pinnacle Point, Klasies River, and Blombos Cave (Matthews et al., 2011, 2020; Nel et al., 2018; Nel and Henshilwood, 2021). Thus, using modern owl pellets from barn owls is a valid sampling strategy to get a representative collection of micromammal species from the area.

These modern micromammal specimens were manually extracted from the owl pellets by carefully teasing the pellets apart with tweezers, separating fur and bone and collecting the osseous material and teeth found in the pellets. No chemicals were used in the process. Before sampling for ZooMS, micromammal bones were taxonomically identified by morphological characteristics of molars, mandibles, maxillae, and dental morphology, following standard methods (Nel, 2013) and with the aid of comparative specimens from Iziko South African Museum in Cape Town, a private collection of comparative samples at the University of Bergen and identification keys developed by Avery (1979) and De Graaff (1981). Morphological analyses for taxonomic determination

were carried out at the Iziko South African Museum in Cape Town, South Africa, and at the University of Bergen, Norway. Modern reference specimens were collected for 14 species: Cape gerbil (*Gerbilliscus afra*), forest shrew (*Myosorex varius*), reddish-grey musk shrew (*Crocodyria cyanea*), lesser dwarf shrew (*Suncus varilla*), grey climbing mouse (*Dendromus melatonis*), Brant's climbing mouse (*Dendromus mesomelas*), African pygmy mouse (*Mus minutoides*), Robert's vlei rat (*Otomys karooensis*), Southern African vlei rat (*Otomys irroratus*), Sloggett's vlei rat (*Otomys sloggetti*), Littledale's whistling rat (*Parotomys littledalei*), Verreux's mouse (*Myomyscus verreuxii*), four-striped grass mouse (*Rhabdomys pumilio*), and Namaqua rock mouse (*Micamelamys namaquensis*). An overview of the specimens and their collection sites are available in [Table S1](#). This list of identified species is not extensive for the area, though the species are all expected to occur in the southern Cape coastal region at present, with exception of *O. sloggetti* and *P. littledalei* (IUCN, 2022).

### 2.1.2. Archaeological specimens

Archaeological micromammal specimens were collected from the section and surface cleanings of the MSA levels at KDS. The stratigraphic provenance of these specimens within the MSA sequence at KDS was determined by association to one or several layers, or to technological periods such as the Howiesons Poort sequence ([Fig. 2](#)). Section and surface cleanings were chosen as our pilot study aimed to establish the feasibility of ZooMS analysis on material from MSA sequences in South Africa. This means that the exact provenance (i.e. layer and in some instances square) within the MSA sequence at KDS is not known for all samples (see [Table S2](#)). While the provenance is not exact, these samples are still valuable and provide general information from the MSA and HP deposits at KDS. Sampled bones include maxillae, mandibles, femurs, humeri, tibiae, ulnae, radii, scapulae, vertebrae, ribs, astragali, calcanei, metatarsals, phalanges, as well as unidentifiable post-cranial fragments. The total weight for the post-cranial samples was 15.14 g while the cranial bone elements weighed 8.38 g. Some of the cranial elements (mandibles and maxillae) were identifiable to species or genus (depending on their fragmentation) by dental morphology ([Table S2](#)). However, some maxillae fragments could only be identified as Muridae, as the fragments did not contain teeth and identification based on alveoli was not possible. In total, 102 bones from across multiple contexts were selected for ZooMS analysis. The individual bones were not weighed prior to analysis. Samples were selected widely across the stratigraphy rather than by element, as NISP and MNI calculations were outside the scope of this pilot study.

## 2.2. Collagen extraction

Entire specimens (archaeological and modern) were used for collagen extraction because of the small size of the microfaunal remains. Collagen was extracted in the ZooMS laboratory of the Max Planck Institute for the Science of Human History (now Max Planck Institute of Geoanthropology), Jena, Germany, using an acid-insoluble approach based upon previously published methods ([Buckley et al., 2009](#); [Welker et al., 2015](#)). The bones were demineralized in 400  $\mu$ l 0.6 M hydrochloric acid (HCl) for 24–72 h. The supernatant was removed after which the samples were washed three times in 200  $\mu$ l 50 mM ammonium bicarbonate pH 8 (AmBic). The samples were then incubated in 200  $\mu$ l 0.1 M sodium hydroxide (NaOH) at room temperature for approximately 5 min and then washed three times in 200  $\mu$ l AmBic. Then, the samples were heated at 65 °C in 100  $\mu$ l AmBic for 1 h 50  $\mu$ l of the resulting supernatant was digested with 0.4  $\mu$ g of trypsin (Pierce™ Trypsin Protease, Thermo Scientific) for 18 h at 37 °C. Subsequent to enzymatic digestion, peptides were purified using C18 ZipTips (Pierce™ C18 Tips, Thermo Scientific) with 0.1% trifluoroacetic acid (TFA) for the washing solution and 50% acetonitrile (ACN), 0.1% TFA for conditioning and elution solutions.

Archaeological samples that did not yield satisfactory results, were re-analysed using an acid-soluble approach following the protocol

described by [Van der Sluis et al. \(2014\)](#). Briefly, the acid supernatant was transferred to a 30 kDa ultrafilter (Sartorius, Vivaspin) and centrifuged at 3700 rpm until the liquid completely passed through the filter. Then, 300  $\mu$ l AmBic was added to the ultrafilter followed by centrifugation. 100  $\mu$ l of AmBic was added to the top of the filter and the proteins were resuspended through pipetting. 50  $\mu$ l was then digested and purified as described above. The exact protocols as applied in this study are described in detail in [Wang et al. \(2021\)](#) and are publicly available on protocols. io ([Brown et al., 2020a, 2020b](#)).

## 2.3. MALDI-TOF-MS

The samples were spotted in triplicate onto an MTP Groundsteel 384-target plate, together with matrix solution ( $\alpha$ -cyano-4-hydroxycinnamic acid of 10 mg/mL in 50% acetonitrile (ACN)/0.1% trifluoroacetic acid (TFA)) and were analysed using an Autoflex Speed LRF Matrix-Assisted Laser Desorption/Ionization Time-of-flight Mass Spectrometer (MALDI-ToF-MS, Bruker Daltonics) with a smartbeam-II laser. A SNAP averaging algorithm was used to obtain monoisotopic masses (C: 4.9384, N: 1.3577, O: 1.4773, S: 0.0417, H: 7.7583). Resulting MALDI spectra of archaeological specimens were visually inspected using Flexanalysis v. 3.4 (Bruker Daltonics) and taxonomically identified using a database of both existing peptide markers for micromammals ([Buckley et al., 2009, 2016, 2018](#); [Prendergast et al., 2017](#)) and peptide markers developed in this study.

## 2.4. LC-MS/MS

For each species, one sample with a good MALDI spectrum was analysed using liquid chromatography with tandem mass spectrometry (LC-MS/MS) to retrieve collagen sequence data. 20  $\mu$ l of the collagen extract was dried down and sent for LC-MS/MS at the Functional Genomics Center Zurich. LC-MS/MS was conducted using a Q-Exactive HF mass spectrometer (Thermo Scientific) coupled with an ACQUITY UPLC M-Class system (Waters AG). Solvent composition at the two channels was 0.1% formic acid for channel A and 0.1% formic acid, 99.9% ACN for channel B. Column temperature was 50 °C. For each sample, 4  $\mu$ l of peptides were loaded on a commercial MZ Symmetry C18 Trap Column (100  $\text{\AA}$ , 5  $\mu$ m, 180  $\mu$ m  $\times$  20 mm, Waters) followed by nanoEase MZ C18 HSS T3 Column (100  $\text{\AA}$ , 1.8  $\mu$ m, 75  $\mu$ m  $\times$  250 mm, Waters). The peptides were eluted at a flow rate of 300 nL/min by a gradient from 5 to 40% B in 120 min and 98% B in 5 min. The column was cleaned after each run with 98% solvent B for 5 min and 98% solvent B was held for 8 min prior to re-establishing loading condition. The mass spectrometers were operated in data-dependent mode performing HCD (higher-energy collision dissociation) fragmentation on the 12 most intense signals per cycle. Full-scan MS spectra (300–1500  $m/z$ ) were acquired at a resolution of 120,000 at 200  $m/z$  after accumulation to a target value (AGC) of 3,000,000, while HCD spectra were acquired at a resolution of 30,000 using a normalized collision energy of 28 (maximum injection time: 50 ms; AGC 10,000 ions). Unassigned singly-charged ions were excluded. Precursor masses previously selected for MS/MS measurement were excluded from further selection for 30 s, and the exclusion window was set at 10 ppm. The samples were acquired using internal lock mass calibration on  $m/z$  371.1012 and 445.1200.

## 2.5. Identification and confirmation of biomarkers

The identification and confirmation of peptide biomarkers was performed following the methodology described in [Richter et al. \(2020\)](#). MALDI spectra of modern reference samples were visually inspected with FlexAnalysis software (Bruker Daltonics) and compared to a list of published peptide markers ([Buckley et al., 2016](#); [Prendergast et al., 2017](#)) to select candidate peptide markers. In addition,  $m/z$  peaks that seemed to be useful to distinguish between taxa were also noted down as candidate peptide markers.

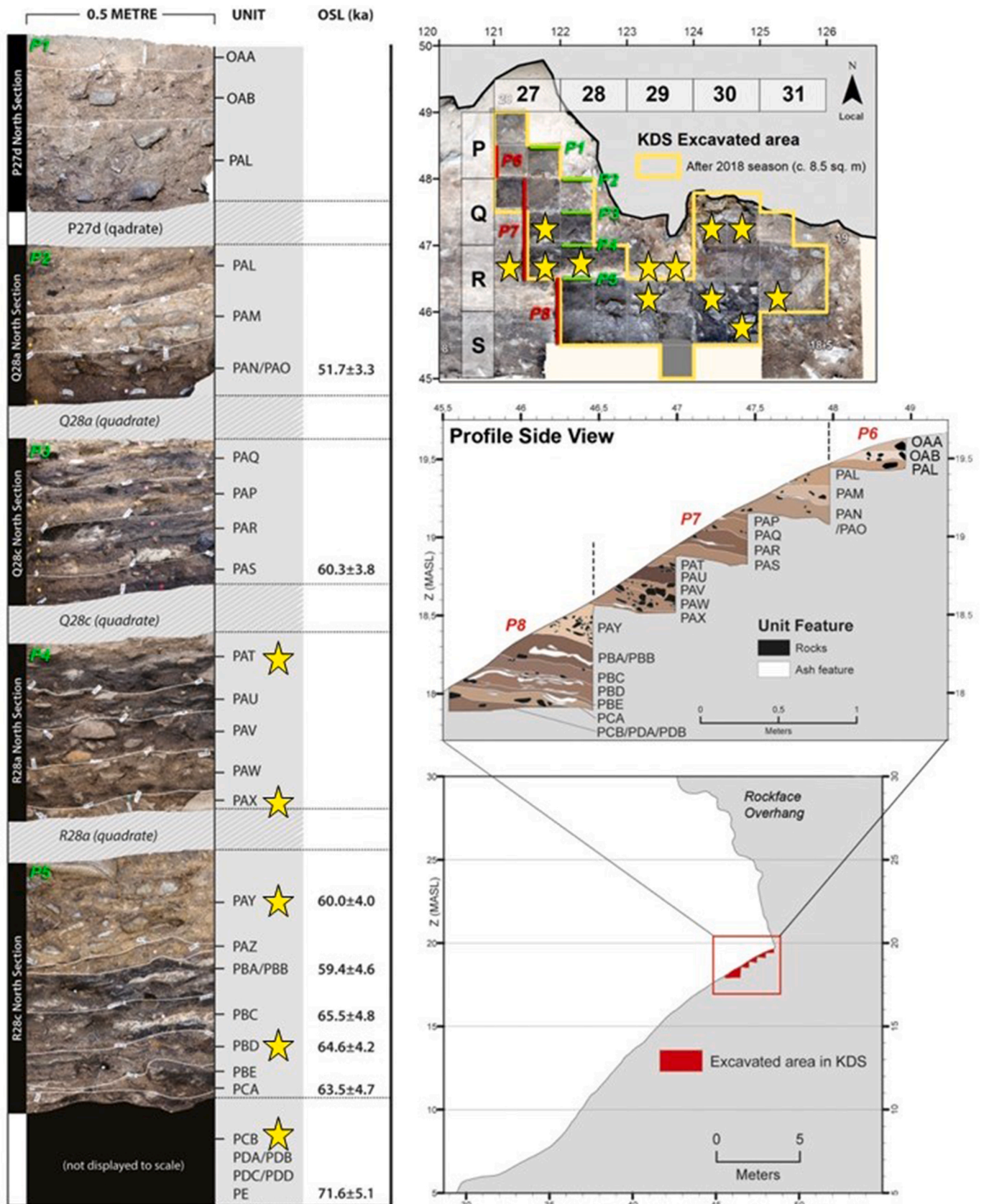


Fig. 2. Klipdrift Shelter: Site map, stratigraphy, and dating. Yellow stars indicate areas and layers which were sampled in this study. Images courtesy of Magnus M. Haaland.

Candidate peptide biomarkers were confirmed using the relevant LC-MS/MS data analysed in a multi-stage approach using Bionic (Protein Metrics Inc., Bern et al., 2012). First, the production spectra were searched against a reference database with all known amino acid sequences of COL1α1 and COL1α2 for mammals, as well as common contaminants. The following parameter settings were used: cleavage sites fully specific C-term R and K; 3 missed cleavages allowed; mass changes: 6 common, 0 rare; common: oxidation on lysine (K), methionine (M), and proline (P), deamidation of asparagine (N) and glutamine (Q); no sequence variations allowed; wildcard search disabled; protein FDR 2%. Masses of published and candidate peptide markers were checked to identify the corresponding amino acid sequences (peptide

PEP2D score lower than 0.01). A focused database was made from the proteins identified in this search. The focused databases from all samples were then combined and duplicates were removed.

Next, species without confirmed sequence data for all candidate markers were re-analysed using an error tolerant search strategy to identify novel sequence variants using the combined focused database. The following parameter settings were used: cleavage sites fully specific C-term R and K; 2 missed cleavages allowed; mass changes: 6 common, 1 rare; common: oxidation on K, M, and P, deamidation on N and Q; rare: all sequence variants allowed; wildcard search disabled; protein FDR 2%. The locations of the peptide markers on the collagen gene were checked and all possible sequence variants and their corresponding

**Table 1**

ZooMS markers for African micromammals included in this study. Naming of peptide markers follows Brown et al. (2021a). Masses in italics are not visible in MALDI spectra but have been observed in MS/MS data. Bolded masses represent key peptide markers that can be used to distinguish between taxonomic groups. Grayed out masses are not useful to make ZooMS identifications.

Subfamily	Genus	Species	Peptide markers								
			COL1α1 508–519	COL1α2 978–990	COL1α2 246–261	COL1α1 311–325	COL1α1 704–720 <sup>b</sup>	COL1α2 484–498	COL1α2 697–713	COL1α2 898–915	
			P1	A	A'	Marker 3 (Buckley et al., 2016)	Marker 2 (Buckley et al., 2016)	B			
<b>Gerbillinae</b>	<i>Gerbilliscus</i>	<i>afra</i>	1105	1187	1203	1267 <sup>a</sup>	1435 <sup>a</sup>	<b>1459</b>	1453	1533	1560 (1576)
<b>Murinae</b>	<i>Mus</i>	<i>minutoides</i>	1105	1187	1203	1267 <sup>a</sup>	<b>1465</b>	1443	1453	1533	1562 (1578)
		<i>Otomys</i>	<i>karoensis</i>	1105	1187	1203	1267 <sup>a</sup>	1451 <sup>a</sup>	1443	1453	1533
		<i>irroratus</i>	1105	1187	1203	1267 <sup>a</sup>	1451 <sup>a</sup>	1443	1453	1533	1560 (1576)
		<i>sloggetti</i>	1105	1187	1203	1267 <sup>a</sup>	1451 <sup>a</sup>	1443	1453	1533	1560 (1576)
	<i>Parotomys</i>	<i>littledalei</i>	1105	1187	1203	1267 <sup>a</sup>	1451 <sup>a</sup>	1443	1453	<b>1501</b>	1560 (1576)
	<i>Myomyscus</i>	<i>verreauxii</i>	1105	<b>1205</b>	<b>1221</b>	1267 <sup>a</sup>	1451 <sup>a</sup>	1443	1453	1533	1560 (1576)
	<i>Rhabdomys</i>	<i>pumilio</i>	1105	1187	1203	<b>1293</b>	1451 <sup>a</sup>	1443	1453	1533	1560 (1576)
	<i>Micaelamys</i>	<i>namaquensis</i>	1105	1187	1203	1267 <sup>a</sup>	1451 <sup>a</sup>	1443	1453	1533	1560 (1576)
<b>Dendromurinae</b>	<i>Dendromus</i>	<i>melatonis</i>	1105	1187	1203	1267 <sup>a</sup>	<b>1465</b>	1443	1453	1533	<b>1574</b> (1590)
		<i>mesomelas</i>	1105	<b>1178</b>	<b>1194</b>	1267 <sup>a</sup>	<b>1465</b>	<b>1459</b>	1453	1533	<b>1574</b> (1590)
<b>Myosoricinae</b>	<i>Myosorex</i>	<i>varius</i>	1105	<b>1205</b>	<b>1221</b>	<b>1253</b>	<b>1465</b>	<b>1473</b>	1453	<b>1501</b>	1592
<b>Crociodurinae</b>	<i>Crociodura</i>	<i>cyanea</i>	1105	<b>1210</b>	<b>1226</b>	1251 <sup>a</sup>	1435 <sup>a</sup>	<b>1459</b>	1453	1533	1592
		<i>Suncus</i>	<i>varilla</i>	1105	<b>1210</b>	<b>1226</b>	<b>1279</b>	1435 <sup>a</sup>	<b>1459</b>	1453	1533

Subfamily	Genus	Species	Peptide markers									
			COL1α2 502–519	COL1α2 292–309	COL1α2 384	COL1α2 793–816	COL1α2 454–483	COL1α1 586–618	COL1α2 664–696			
			C	P2		D	E	F	F'			
<b>Gerbillinae</b>	<i>Gerbilliscus</i>	<i>afra</i>	1566	1578	1182 (2098)	2145 <sup>a</sup>	2806 <sup>a</sup>	<b>2841</b>	<b>2857</b>	<b>2849</b>	<b>2865</b>	
<b>Murinae</b>	<i>Mus</i>	<i>minutoides</i>	1570	1566	1182 (2098)	2143	x	2925, 2941, 2957 <sup>c</sup>		2923	2939	
		<i>Otomys</i>	<i>karoensis</i>	1566	1592	1182 (2098)	x	2836	2925, 2941, 2957 <sup>c</sup>		2923	2939
		<i>irroratus</i>	1566	1592	1182 (2098)	2143	2836	2925, 2941, 2957 <sup>c</sup>		2923	2939	
		<i>sloggetti</i>	1566	1592	1182 (2098)	2143	2836	2925, 2941, 2957 <sup>c</sup>		2923	2939	
	<i>Parotomys</i>	<i>littledalei</i>	1566	1592	x	2143	2836	2925, 2941, 2957 <sup>c</sup>		2923	2939	
	<i>Myomyscus</i>	<i>verreauxii</i>	1566	1592	1182 (2098)	2143	2836	2925, 2941, 2957 <sup>c</sup>		2923	2939	
	<i>Rhabdomys</i>	<i>pumilio</i>	1566	1592	1182 (2098)	2143	2836	2925, 2941, 2957 <sup>c</sup>		2923	2939	
	<i>Micaelamys</i>	<i>namaquensis</i>	1566	1592	1182 (2098)	2143	2836	2925, 2941, 2957 <sup>c</sup>		2923	2939	
	<b>Dendromurinae</b>	<i>Dendromus</i>	<i>melatonis</i>	1566	1578	1182 (2098)	x	x	<b>2869</b>	<b>2885</b>	<b>2849</b>	<b>2865</b>
			<i>mesomelas</i>	1566	1578	1182 (2098)	x	x	<b>2869</b>	<b>2885</b>	<b>2849</b>	<b>2865</b>
<b>Myosoricinae</b>	<i>Myosorex</i>	<i>varius</i>	1550	x	x	2161 <sup>a</sup>	2836	2911	2927	<b>2879</b>	<b>2895</b>	
<b>Crociodurinae</b>	<i>Crociodura</i>	<i>cyanea</i>	x	x	<b>2118</b>	x	2822 <sup>b</sup>	<b>2869</b>	<b>2885</b>	<b>2881</b>	<b>2897</b>	
		<i>Suncus</i>	<i>varilla</i>	x	x	<b>2118</b>	x	<b>2866</b>	<b>2869</b>	<b>2885</b>	<b>2895</b>	2911

<sup>a</sup> Within each marker, masses that are 16 Da apart cannot be clearly separated using MS/MS. Therefore, they cannot be distinguished from each other, but can be distinguished from other masses of the same marker.

<sup>b</sup> Even though  $m/z$  1443 and  $m/z$  1459 are 16 Da apart, the peptides visible in the MALDI have 2 proline oxidations each and can be clearly separated in MS/MS data. This marker can thus be useful to make ZooMS identifications, although has to be used with caution.

<sup>c</sup> Two sets of sequences were identified in these taxa. These sequences have the same  $m/z$  values but a different number of oxidations. These markers are indistinguishable in MALDI spectra, and have therefore been grouped together.

masses were recorded (peptide PEP2D score lower than 0.01).

Other proteins in the samples were identified by searching the MS/MS spectral data against a database composed of Swissprot (downloaded 03.04.2020) and the proteomes of *Mus musculus* (UP000000589), *Myotis lucifugus* (UP000001074), *Cricetulus griseus* (UP000001075), *Canis lupus familiaris* (UP000002254), *Equus caballus* (UP000002281), *Rattus norvegicus* (UP000002494), *Callithrix jacchus* (UP000008225), *Sus scrofa* (UP000008227), *Myotis brandtii* (UP000052978), *Mesocricetus auratus* (UP000189706), *Orcinus orca* (UP000242909), using the following parameter settings: cleavage sites fully specific C-term R and K; 3 missed cleavages allowed; mass changes: 2 common, 1 rare; common: oxidation on K, M, and P, deamidation on N and Q; rare: pyro-Glu on N-term E and Q, ammonia-loss on N-term C; no sequence variations allowed; wildcard search disabled; protein FDR 2%. A focused database was made from the proteins identified in this search. The focused databases from all samples were then combined and duplicates were removed.

The results of the first three searches were used to create a new database consisting of (i) the COL1 $\alpha$ 1 and COL1 $\alpha$ 2 sequences of the original reference database, (ii) all sequence variants found in the error tolerant search, (iii) all proteins identified in the whole proteome validation, and (iv) common contaminants (database uploaded to ProteomeXchange). The MS/MS data was then analysed using this database and the same parameter settings as the first non-error tolerant search. Only peptides with at least three peptide spectral matches with a PEP2D score lower than 0.01, were considered confirmed. This resulted in a list of confirmed peptide markers and corresponding peptide sequences.

### 3. Results

The modern reference samples yielded high-quality MALDI and MS/MS spectral data, and collagen has been identified as the main protein component in all samples (Table S3). The newly acquired ZooMS peptide markers are presented in Table 1, and the corresponding peptide sequences are presented in Table 2 (see also Figs. S1–S18). All micro-mammal species studied share two peptide markers: COL1 $\alpha$ 1 508 (P1) at  $m/z$  1105, and COL1 $\alpha$ 2 484 (B) at  $m/z$  1453. We were unable to locate the COL1 $\alpha$ 2 757 (G) marker peptide in either the MALDI or the MS/MS spectral data and it is therefore not reported in Tables 1 and 2. The other six regularly reported ZooMS markers, peptide markers COL1 $\alpha$ 1 311–325 and COL1 $\alpha$ 1 704–720 previously reported for murine rodents (Buckley et al., 2016), and the peptide marker COL1 $\alpha$ 2 898 useful for distinguishing within Bovidae (Coutu et al., 2021; Janzen et al., 2021) all show variation. Furthermore, we report four new peptide markers which combined allow for genus-level distinctions to be made between the micromammals included in this study (Table 1, Fig. 3).

#### 3.1. Taxonomic resolution using ZooMS

We analysed samples from five subfamilies of which two subfamilies are represented by one species each (Gerbillinae and Myosoricinae), one subfamily is represented by two species in the same genus (Dendromurinae), and two subfamilies are represented by more than one genus (two genera each with one species represented for Crocidurinae; six genera with 8 species from Murinae). All subfamilies included in this study can be distinguished from each other. In Crocidurinae both genera can be separated. In Murinae all three species of *Otomys* and one species of *Micaelamys* studied are indistinguishable from each other, but can be differentiated from the other four genera studied. Within Dendromurinae, *D. melatonis* and *D. mesomelas* can be distinguished.

The additional markers identified in this study allow for the separation of *M. minutoides* from *R. pumilio* and *P. littledalei* from the *Otomys*/*Micaelamys* group (Table 1). In addition, the new markers provide more options for confirmation of taxonomic resolution which is important as not all markers are visible in every sample, especially when collagen is poorly preserved as is often the case in African zooarchaeological assemblages.

**Table 2**

Peptide sequences corresponding to ZooMS markers presented in Table 1. Naming of peptide markers follows Brown et al. (2021a). Masses in brackets represent the mass of the peptide with an additional oxidation. Differences between sequences are bolded and underlined.

Marker		Sequence	Mass (m/z)
COL1 $\alpha$ 1 508–519	P1	GVQPPGPAGPR	1105
COL1 $\alpha$ 2 978–990	A	<u>SGQ</u> PGPVGPA <u>GV</u> R <u>SGHPG</u> PGPVGPA <u>GV</u> R <u>SGHPGT</u> VPAG <u>IR</u> <u>TGQ</u> PGTVGPA <u>IR</u>	1178 (1194) 1187 (1203) 1205 (1221) 1210 (1226)
COL1 $\alpha$ 2 246–261		GIPGPA <u>GAAGASG</u> PR  GIPGP <u>VGAAGASG</u> AR GIPGP <u>VGAAGATG</u> AR GIPGP <u>VGAAGASG</u> PR GIPGP <u>VGAAGATG</u> PR GEPGPA <u>GLGPPG</u> ER	1251  1253 1267 1279 1293 1435
COL1 $\alpha$ 1 311–325		GEPG <u>PSGLP</u> PPGER GEPG <u>PTGLP</u> PPGER GA <u>AGPPG</u> ATGFPGAAGR	1451 1465 1443
COL1 $\alpha$ 1 704–720		GS <u>AGPPG</u> ATGFPGAAGR GT <u>AGPPG</u> ATGFPGAAGR GLPGE <u>FLG</u> PAGPR	1459 1473 1453
COL1 $\alpha$ 2 484–498	B	GDGGPPG <u>VTG</u> FPGAAGR	1501
COL1 $\alpha$ 2 697–713		GDGGPPG <u>MTG</u> FPGAAGR GEPGPA <u>GSV</u> PGV <u>GA</u> VGPR	1533 1560
COL1 $\alpha$ 2 898–915		GEPGPA <u>GSV</u> PGT <u>GA</u> VGPR GEPG <u>PSG</u> PV <u>LAG</u> AVGPR GEPGPA <u>GA</u> VGPV <u>GA</u> FGR G <u>PP</u> GESGAAG <u>PSG</u> PLGSR	1562 (1578) 1574 (1590) 1592 1550
COL1 $\alpha$ 2 502–519	C	G <u>PP</u> GESGAAG <u>PSG</u> PLGSR G <u>TP</u> GESGAAG <u>PSG</u> PLGSR GSPGE <u>AGS</u> AGPA <u>G</u> PPGLR	1566 1570 1566
COL1 $\alpha$ 2 292–309	P2	GSPGEP <u>GS</u> AGP <u>G</u> PPGLR GSPGEP <u>GS</u> AGP <u>A</u> PPGLR EGP <u>V</u> GLPGIDGR EGP <u>V</u> GLPGIDGR/PGPIG <u>P</u> AGPR EGP <u>M</u> GLPGIDGRPGPIG <u>P</u> AGTR	1578 1592 1182 2098 2118
COL1 $\alpha$ 2 793–816	D	GLPGIAG <u>AL</u> GEPG <u>P</u> LGIA <u>G</u> PPGAR GLPGIAG <u>SL</u> GEPG <u>P</u> VGIAGPPGAR GLPGIAG <u>SV</u> GEPG <u>P</u> LGI <u>S</u> GPPGAR	2143 2145 2161
COL1 $\alpha$ 2 454–483	E	GEQGPAGPPGFQGLPG <u>PSGA</u> AGEVGKPGER GEQGPAGPPGFQGLPG <u>PSGT</u> AGEVGKPGER GEQGPAGPPGFQGLPG <u>PSGTT</u> AGEVGKPGER GLTGPIGPPGAG <u>AG</u> DKGET <u>G</u> PSGPA <u>G</u> PTGAR	2822 2836 2866 2841
COL1 $\alpha$ 1 586–618	F	GLTGPIGPPGAG <u>AG</u> DKGET <u>G</u> PSGPA <u>G</u> PTGAR GLTGPIGPPGAG <u>AG</u> DKGET <u>G</u> PSGPA <u>G</u> PTGAR GLTGPIGPPGAG <u>AG</u> DKGET <u>G</u> PSGPA <u>G</u> PTGAR GLTGPIGPPGAG <u>AG</u> DKGET <u>G</u> PSGPA <u>G</u> PTGAR GLTGPIGPPGAG <u>AG</u> DKGET <u>G</u> PSGPA <u>G</u> PTGAR	(2857) 2869 (2885) 2883 (2899) 2911 (2927) 2941 (2957)
COL1 $\alpha$ 2 664–696		GPKG <u>ENG</u> V <u>VP</u> G <u>AG</u> PVGAAGPSGPN <u>GG</u> PPV <u>G</u> GR GPKG <u>ENG</u> V <u>VP</u> G <u>AG</u> PVGAAGPSGPN <u>GG</u> PPA <u>GS</u> R	2849 (2865) 2879 (2895)

(continued on next page)

Table 2 (continued)

Marker	Sequence	Mass ( <i>m/z</i> )
	GPKGENGVVGPVGAAGPSGPNPPGAGSR	2881 (2897)
	GPKGENGVIGPTGPVGAAGPSGPNPPGAGSR	2895 (2911)
	GPKGENGVIGPTGPVGAAGPSGPNPPGPGVGSR	2923 (2939)

### 3.2. Notes on particular markers

As more markers are defined, overlapping or indistinguishable markers become more commonly observed (Janzen et al., 2021; Peters et al., 2021). Several markers contain sequences for which care must be taken in interpretations. COL1 $\alpha$ 2 384 is only identified in some species. In addition, one of the peptides is frequently observed in the MALDI at both *m/z* 1182 (EGPVGLPGIDGR) and with one missed cleavage at *m/z* 2098 (EGPVGLPGIDGRPGPIGAGPR). The peak at *m/z* 2911 could be from either COL1 $\alpha$ 1 586 (F) in *M. varius*, or COL1 $\alpha$ 2 664 in *S. varilla*. Similarly, a peak at *m/z* 2895 in COL1 $\alpha$ 2 664–696 could either represent *S. varilla*, or *D. mesomelas* (with an additional oxidation). Therefore, these *m/z* values should be used with caution and ideally only when present together with their counterpart, as it could otherwise lead to confounding results.

Collagen has frequent variable oxidations of proline which correspond to a difference in 16 Da between versions of the same peptide; a phenomenon that is well described for markers COL1 $\alpha$ 2 978 (A), COL1 $\alpha$ 1 586 (F), COL1 $\alpha$ 2 757 (G) (Buckley et al., 2009). However, a common amino acid variation in collagen, alanine vs. serine, also corresponds to a mass difference of 16 Da. While MS/MS spectral data can be used to distinguish between a proline oxidation and a single amino acid difference between alanine and serine, this is not possible in MALDI data. Therefore, in some cases peptide markers cannot be distinguished in the MALDI. For example, COL1 $\alpha$ 1 311 has a version at *m/z* 1435 (GEPGPAGLPGGPGER) present in Gerbillinae and Crocidurinae and a version at *m/z* 1451 (GEPGPSGLPGGPGER) present in Murinae (except *M. minutoides*) where each peptide has three oxidized prolines. However, in the MS/MS data both peptides are identified with two (*m/z* 1419 and *m/z* 1435 respectively) and four oxidized prolines (*m/z* 1451 and *m/z* 1467 respectively). While it is unusual to see the peptides with two or four oxidized prolines in the MALDI data, it cannot be excluded entirely. Therefore, COL1 $\alpha$ 1 311 at *m/z* 1435 and *m/z* 1451 cannot be used as diagnostic to separate Gerbillinae/Crocidurinae from Murinae. It can however be used to differentiate these groups from Dendromurinae/Myosoricinae/*M. minutoides* with *m/z* 1465. This is also the case for COL1 $\alpha$ 2 246, COL1 $\alpha$ 2 793 (D), and COL1 $\alpha$ 2 454 (E) as indicated in Table 1 (marked with \*). One exception is COL1 $\alpha$ 1 704, which also has two sequences corresponding to a 16 Da difference: *m/z* 1443 (GAAGPPGATGFPGAAGR) and *m/z* 1459 (GSAGPPGATGFPGAAGR). Each of these peptides have two oxidized prolines. MS/MS spectral data shows that both of these proline oxidations are fixed, meaning that both peptides always have two oxidized prolines and not one or three. Therefore, these can be used as diagnostic peaks, albeit with caution.

Finally, many peptides are visible in the *m/z* 1500–1600 region in the MALDI. For many of the peptides in this region, the MS/MS analysis was able to uniquely identify the marker peptides. Even though in many cases we were able to identify the *m/z* peak in the MALDI spectrum corresponding to these peptide sequences, the large number of overlapping marker and non-marker collagen peptides in this mass range make differentiating between unique peaks difficult. In addition, many peaks are composed of more than one peptide similar to that of the well identified *m/z* 3017 in Bovidae (Janzen et al., 2021). For COL1 $\alpha$ 2 697, *m/z* 1501 is distinctive and therefore can be used for taxonomic identification for *P. littledalei* and *M. varius*, but *m/z* 1533 cannot be used as it

is composed of more than one peptide and visible in all species. Likewise, COL1 $\alpha$ 2 898 can only be used to identify *Dendromus* at *m/z* 1574/1590. Using only one version of a peptide for an identification when it is present has been shown to be useful to make positive identifications, as for *Cervus elaphus* (Jensen et al., 2020). In the case of COL1 $\alpha$ 2 502 (C) and COL1 $\alpha$ 2 292 (P2) we were able to identify the masses of the peptides corresponding to the MS/MS spectral data, but the overlap in the region is too great to reliably use them for any identifications.

### 3.3. ZooMS analysis at Klipdrift shelter

We analysed a total of 102 archaeological bone fragments from the section and surface cleanings of the MSA layers at KDS (Table 3). Twenty-eight samples had collagen peptides visible in the MALDI (27% success rate), though variation in success rates within the various site contexts range from 0 to 92%. It is especially worth noting that section cleanings of the Howiesons Poort layers dated between  $65.5 \pm 4.8$  ka and  $59.4 \pm 4.6$  ka (Henshilwood et al., 2014) have a success rate of 92%.

Of the 28 samples with sufficient collagen preservation, 23 could be taxonomically identified to species, genus, or subfamily level using the peptide markers developed in this study (Table S2). Eighteen of these could be identified to only subfamily level: 9 were assigned as Gerbillinae, 2 as Gerbillinae/Crocidurinae, 6 as Murinae, and 1 as Myosoricinae. An additional, 5 specimens were identified to species- or genus-level (*M. minutoides* (n = 3), *D. melatonis* (n = 1), and *Rhabdomys* sp. (n = 1)) (Fig. 4). The five other samples did not match the marker profiles for any taxa currently available in the ZooMS reference database, which means they currently are unidentifiable. Two of these unidentifiable specimens appear to be from the same taxonomic group and have COL1 $\alpha$ 1 508–519 (P1) at *m/z* 1105 which is indicative of most placental mammals. They thus likely derive from a micromammal which is not currently represented in the reference database. One of these unidentifiable specimens can be tentatively assigned as bird/reptile based on the presence of peptide marker COL1 $\alpha$ 1 508–519 (P1) at *m/z* 1162 (Harvey et al., 2019). The other two have lower quality data and do not match any other taxa in the current database. They are thus unidentifiable.

Our ZooMS-identified micromammal assemblage is too small for a reliable assessment of biodiversity, the latter often estimated using various indices such as species richness (i.e. number of taxa identified), general diversity (number of individuals per species) and evenness of the assemblage. With a greater number of identified small mammals, and combined with the micromammal zooarchaeological assemblage, reconstructing the palaeoenvironmental conditions during the Howiesons Poort period is feasible with the foundation work presented here.

## 4. Discussion

### 4.1. Peptide marker development for South African micromammals

The set of peptide markers developed in this study broadly agrees with previously published markers for *Gerbilliscus validus*, *M. minutoides*, and *Otomys tropicalis* (Prendergast et al., 2017). However, complete marker profiles for these taxa were not established, and they had not been confirmed with LC-MS/MS analysis previously. Interestingly, our work identifies several differences between the peptide marker profiles of *M. minutoides* and the previously published marker profile of *M. musculus* (Buckley et al., 2009, 2016). Raw MS/MS data for *M. musculus* is not publicly available from these studies, rendering it impossible to directly compare our results to the previously published markers to disentangle the nature of the observed differences. We thus stress the importance of making raw MALDI spectra and MS/MS data publicly available upon publication so that data can be compared, reproduced and confirmed independently.

The identification of South African micromammals with ZooMS does not come without caveats. The main limitation is that some taxa (e.g.



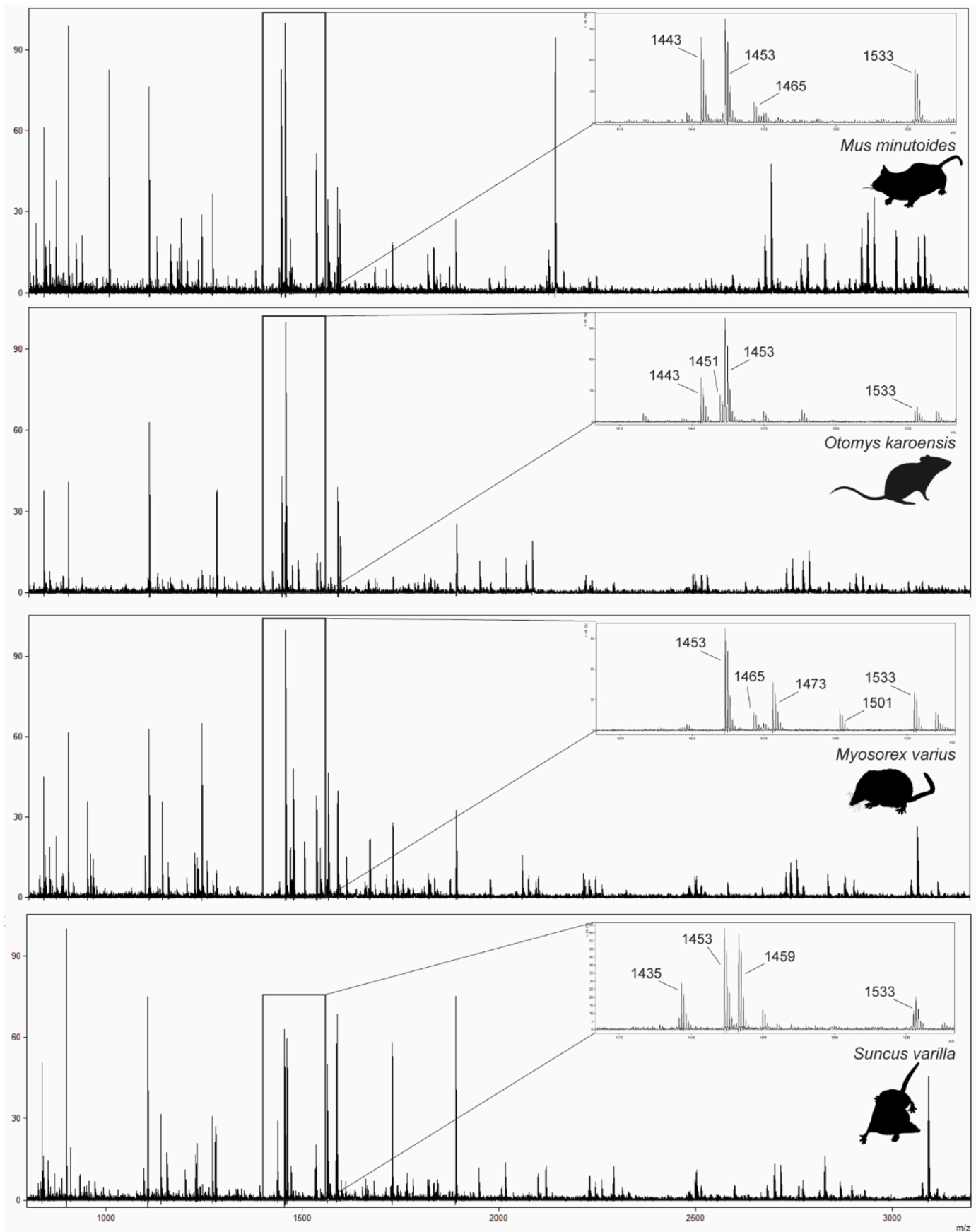
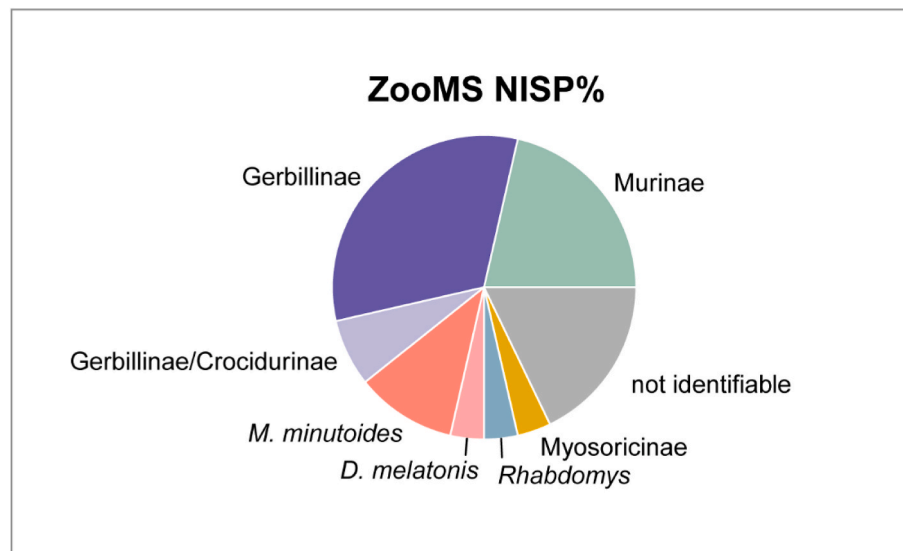


Fig. 3. Examples of MALDI spectra for some of the rodent species included in this study. The zoomed-in panels represent  $m/z$  1400–1550. Some differences in the peptide fingerprints in this mass range between taxa are highlighted.

**Table 3**  
Overview of ZooMS success rates of micromammal identification from KDS.

Square	Provenance	Year Excavated	Lab IDs	Number of bone fragments extracted	Number IDable	Percent Success
R30a	Surface cleaning above PAX	2012	KDS-62 to KDS-77	17	6	35%
R31a	Surface above PAX	2012	KDS-84 to KDS-92	12	1	8%
Q27d	Section cleaning PAX	2013	KDS-5 to KDS-13	6	3	50%
R29c	Section cleanings of PBD	2012	KDS-33 to KDS-43	9	1	11%
R27a, R27b, R28a, R29a, R29b	Section cleaning of PAY, PAX, and PAT	2013	KDS-18 to KDS-32	21	2	10%
Q30c/d	Section cleaning	2013	KDS-78 to KDS-80	8	2	25%
S30b	PCB section cleaning	2012	KDS-101 to KDS-106, KDS-111	9	0	0%
R27b	Section cleaning	2013	KDS-1 to KDS-4	8	2	25%
Not listed	HP section cleaning	2014	KDS-44 to KDS-61	12	11	92%
<b>Total</b>				<b>102</b>	<b>28</b>	<b>27%</b>



**Fig. 4.** ZooMS results for archaeological samples.

*Otomys*) can only be identified to genus-level using ZooMS, while others can only be differentiated on the basis of a single peptide marker. Meanwhile *Otomys* can be identified to species based on dental morphological characteristics of the lower first molar or upper third molar provided that these teeth are present in the archaeological assemblage. Mandibles or maxillae without dental remains can be identified to genus-level for *Otomys*. For other species, these elements can be identified to species-level based on alveoli characteristics. However, this is hardly practiced for archaeological assemblages due to fragmentation. ZooMS can provide taxonomic identifications in these instances, but it requires high-quality spectral data. Collagen thus needs to be well-preserved; something that is not always the case, especially in older deposits. Ways to overcome this is the large-scale prescreening of bone assemblages with non-destructive approaches such as FTIR (Pothier Bouchard et al., 2019; Kontopoulos et al., 2020) or NIR (Sponheimer et al., 2019; Lugli et al., 2021).

Despite these caveats, collagen diversity appears to be greater in micromammals than in large mammals, which allows for a higher taxonomic resolution with ZooMS. For large mammals, ZooMS can generally be used to differentiate between subfamilies, tribes and subtribes (e.g. Janzen et al., 2021), although exceptions exist where genus- and species-level identifications are possible (e.g. Peters et al., 2021). In contrast, ZooMS allows for genus-level distinctions for the majority of the micromammals included in this study, with resolution possible up to species-level for some taxa, between *D. melatonis* and *D. mesomelas*, for example. These species presently occur in the coastal

region of South Africa (Child and Monadjem, 2016a, 2016b). Both taxa prefer grassland and savanna habitats, though *D. mesomelas* may also be found in forest/grassland mosaic habitats (Child and Monadjem, 2016b). Morphological identification of these species in an archaeological assemblage can be tricky. Due to their delicate nature they are often subjected to fragmentation, and the small size of their molars (0.9–1.6 mm for the largest tooth (first upper molar)), accurate identification depends on a few discernible morphological markers on the upper/lower first molars. So, while this pilot study provides an initial effort to develop a ZooMS reference dataset for South African micromammals, it also highlights the need for further work to build a robust methodological framework and reference dataset for the analysis of micromammal material from archaeological sites in southern Africa with ZooMS.

#### 4.2. Insights at KDS

As pointed out earlier in section 3.3, the number of archaeological samples analysed in this study is too small to make a rendition of environmental conditions. Furthermore, due to the material deriving from section and surface cleanings, provenances are in general categories such as MSA deposits and HP deposits. With these limitations in mind, our results still provide general which can be related to other palaeoenvironmental data from KDS. Two species were identified through ZooMS analysis: *D. melatonis* and *M. minutoides*. *M. minutoides* is a versatile species with an extensive range throughout Sub-Saharan

Africa (Monadjem et al., 2015). *D. melanotis* occurs in grasslands and savanna, although it is common in a variety of habitats (Child and Monadjem, 2016a). Climbing mice, such as *D. melanotis*, are primarily associated with tall grasses (Skinner and Chimimba, 2005). The occurrence of the species at KDS in the HP layers is in line with the terrestrial large mammal faunal composition of the youngest HP layers, which points to the development of a grassland-dominated ecosystem (Reynard et al., 2016a). Analyses of stable isotopes from ostrich eggshell at KDS show  $\delta^{13}\text{C}$  values within the range of  $\text{C}_4$  plants and suggests a dominance of  $\text{C}_4$  grasses near KDS (Roberts et al., 2016). Reynard et al. (2016a) have found that there is a significant increase in the proportion of large mammal grazers in the HP at KDS, while declining in the post-HP layers (PAY/PAZ) (see Fig. 2 for stratigraphic association).

Nine samples were assigned as Gerbillinae with ZooMS, two of which were morphologically identified as *G. afra* (Table S2). This species is associated with sandy soils necessary for burrowing, indicating the presence of alluvial conditions in proximity to KDS. Both Henshilwood et al. (2014) and Reynard et al. (2016b) have noted that the presence of Cape dune mole rats (*Bathyergus suillus*) in PAZ and PAY (Fig. 2) and their absence in all other layers, could indicate a change in the local environment to more sandy conditions, possibly associated with dune activity or exposed sea sand during the post-HP. The occurrence of Gerbillinae in both HP and post-HP layers, as well as morphological identification of the African mole rat (*Cryptomys hottentotus*) in HP deposits (Table S2), suggests that alluvial conditions suitable for burrowing were also present during the HP. Murinae, Myosoricinae, *Rhabdomys* sp., and Gerbillinae/Crocidurinae were also identified with ZooMS. However, these identifications could entail a range of possible species and thus require further refinement for the purpose of palaeoenvironmental reconstruction.

#### 4.3. ZooMS as a zooarchaeological tool for micromammal assemblages

At archaeological sites, micromammal density throughout a sequence can vary greatly, especially in confined sites, such as caves and shelters where humans and predators of micromammal prey are not likely to have occupied the space simultaneously (Nel, 2013; Nel and Henshilwood, 2016, 2021; Nel et al., 2018). The small amount of bone material needed for ZooMS analyses enables information of species composition from layers in an archaeological sequence where micromammals are low in representation by standard MNI calculations. This would result in more robust datasets from entire archaeological sequences. This data can subsequently be used to more accurately examine biodiversity trends, shed light on local environmental and climatic conditions and variations therein through time, and improve our knowledge of species geographic ranges, which are unclear for many micromammal species (Matthews et al., 2020; Matthews and Nel, 2021; Nel and Henshilwood, 2021).

ZooMS also has the potential to increase the number of identified species and/or improve assessment of proportional abundance of species in an archaeological assemblage, especially when used as a supplement to morphological identifications (Buckley et al., 2018). However, further work is also needed to better integrate ZooMS results into existing faunal metrics. Micromammals hold particular promise in this regard, since ZooMS analysis of archaeological micromammal bone fragments is relatively time efficient compared to morphological identification, especially for postcranial elements. Although the minimum number of individuals (MNI) is generally estimated through the presence of craniodental remains, the inclusion of metrics for postcranial remains could enable greater efficiency in MNI counts. Furthermore, ZooMS enables more detailed reconstructions of the taxonomic composition of the faunal assemblage, by presence-absence of specific taxa that can potentially reveal new species, for example. ZooMS also has the potential to nuance variations in relative abundances of species estimated by standard MNI calculations. A particularly interesting target in this regard are limb bones. These are easily quantifiable, frequently

recovered from archaeological assemblages, and less prone to fragmentation which would render the skeletal element unidentifiable. Establishing this methodology in the future could prove to be more efficient than traditional morphological identification of micromammal remains, especially for sites with large quantities of micromammal material.

## 5. Conclusions

The results from this feasibility study show that it is possible to successfully undertake ZooMS analysis of archaeological micromammal bone assemblages from South Africa dating to the MSA (Henshilwood et al., 2014), although preservation is variable between the contexts sampled. The excellent preservation of collagen in some of the sampled deposits, most notably in the Howiesons Poort section cleanings, might also reflect the sample collection methods employed. These samples were collected immediately following the collection of sediment blocks for micromorphology, and were thus not exposed to the surface as long as other section and surface cleanings.

Furthermore, we have successfully established ZooMS peptide markers for 14 micromammal species, which can be used in the future to characterize micromammal assemblages in southern Africa. Micromammal remains are notably difficult to identify, with dental morphology often providing the only way to taxonomically identify remains. However, high fragmentation rates, such as those observed at KDS (Nel pers. obs., Henshilwood et al., 2014; Reynard et al., 2016b), can make this a complicated and time-consuming endeavor, sometimes fully preventing the possibility to make morphological identifications. ZooMS analysis can overcome these issues, and thus has the potential to elaborate on presence/absence of specific taxa and increase taxonomic sample size at archaeological sites. The method thus holds significant promise for future applications at other LSA and MSA sites in southern Africa, although we recognize that additional peptide markers still need to be developed for other micromammal taxa that were not included in this study.

## Funding statement

THN, CSH and KvN have been funded by the Research Council of Norway through its Centres of Excellence funding scheme, SFF Centre for Early Sapiens Behaviour (SapienCE), project number 262618. CP was supported by the Max Planck Society. CSH was partially funded for this research by a South African National Research Foundation Research Chair (SARChI) at the University of the Witwatersrand, South Africa. This work received funding from the ERC under the European Union's Horizon 2020 Research and Innovation Programme grant agreement no.715069 (FINDER) to KD.

## Ethics statement

Permits for export of archaeological material were granted by Heritage Western Cape (Permit no.1901080AS0121E) and South African Heritage Resource Agency (Permit no.2896 KDS-MICROFAUNA-CASEID13400).

## Data accessibility statement

MALDI-ToF-MS data for modern reference specimens (<https://doi.org/10.5281/zenodo.7711119>) and archaeological specimens (<https://doi.org/10.5281/zenodo.7711194>) have been uploaded to Zenodo. MS/MS data files are available at ProteomExchange record PXD040129 and were uploaded through MassIVE (MSV000091290). The files are available for download with an FTP client using the download link: <ftp://MSV000091290@massive.ucsd.edu>.

## Author contributions

T.H.N.: Conceptualization, Data curation, Formal analysis, Investigation, Methodology, Project administration, Resources, Visualization, Writing – original draft, writing-review and editing; C.P.: Data curation, Formal analysis, Investigation, Methodology, Visualization, Writing – original draft, writing-review and editing; K.K.R.: Data curation, Formal analysis, Investigation, Writing – original draft, writing-review and editing; C.H.: Funding acquisition, writing-review and editing; K.v.N.: Conceptualization, Project administration, Resources, Supervision, writing-review and editing; K.D.: Conceptualization, Funding acquisition, Investigation, Project administration, Supervision, writing-review and editing.

All authors gave final approval for publication and agreed to be held accountable for the work performed therein.

## Declaration of competing interest

The authors declare that they have no known competing financial interests or personal relationships that could have appeared to influence the work reported in this paper.

## Data availability

The data is uploaded to Zenodo and ProteomExchange. DOI links are included in a data availability section in the manuscript

## Acknowledgements

Collection of owl pellets in the De Hoop Nature Reserve and at Potberg was kindly facilitated with the permission and help of Cape Nature and their staff. Margaret Avery generously shared valuable information of the location of these roosting sites, while Ole Fredrik Unhammer kindly assisted THN with collection. Special thanks to the U3A Bird Group in Still Bay and its leader Johan van Rooyen for the help in collecting owl pellets and the landowner Annamarié Barnard for allowing access to Witels Farm. Thalassa Matthews and Margaret Avery are thanked for sharing their private comparative micromammal collections. The Iziko South African Museum in Cape Town, South Africa, is thanked for facilitating the morphological analyses and for use of their comparative collection. Samantha Mienies kindly assisted with processing pellets, permit applications and shipping material. Finally, we would like to thank Sandra Hebestreit for technical assistance with ZooMS extractions.

## Appendix A. Supplementary data

Supplementary data to this article can be found online at <https://doi.org/10.1016/j.quascirev.2023.108380>.

## References

- Andrews, P., 1990. *Owls, Caves and Fossils: Predation, Preservation and Accumulation of Small Mammal Bones in Caves, with an Analysis of the Pleistocene Cave Faunas from Westbury-Sub-Mendip*. University of Chicago Press, Somerset, UK. Chicago.
- Avery, D.M., 1979. Upper Pleistocene and Holocene Palaeoenvironments in the Southern Cape: the Micromammalian Evidence from Archaeological Sites. University of Stellenbosch, Stellenbosch.
- Avery, D.M., 1981. Micromammals as palaeoenvironmental indicators and an interpretation of the late quaternary in the southern Cape Province, South Africa. *Ann. S. Afr. Mus.* 85, 183–374.
- Avery, D.M., 1992. Ecological data on micromammals collected by barn owls *Tyto alba* in the west coast national park, South Africa. *Isr. J. Zool.* 38, 385–397. <https://doi.org/10.1080/00212210.1992.10688685>.
- Avery, D.M., 2002. Taphonomy of micromammals from cave deposits at Kabwe (broken hill) and twin rivers in Central Zambia. *J. Archaeol. Sci.* 29, 537–544. <https://doi.org/10.1006/jasc.2001.0749>.
- Avery, D.M., Avery, G., Palmer, N.G., 2005. Micromammalian distribution and abundance in the western Cape Province, South Africa, as evidenced by barn owls *Tyto alba* (Scopoli). *J. Nat. Hist.* 39, 2047–2071. <https://doi.org/10.1080/00222930500044631>.
- Bern, M., Kil, Y.J., Becker, C., 2012. Byonic: advanced peptide and protein identification software. *Current Protocols in Bioinformatics* 40. <https://doi.org/10.1002/0471250953.bi1320s40>, 13.20.11–13.20.14.
- Bradfield, J., Forsman, T., Spindler, L., Antonites, A.R., 2019. Identifying the animal species used to manufacture bone arrowheads in South Africa. *Archaeological and Anthropological Sciences* 11, 2419–2434. <https://doi.org/10.1007/s12520-018-0688-5>.
- Bradfield, J., Kitchener, A.C., Buckley, M., 2021. Selection preferences for animal species used in bone-tool-manufacturing strategies in KwaZulu-Natal, South Africa. *PLoS One* 16, e0249296. <https://doi.org/10.1371/journal.pone.0249296>.
- Brown, S., Hebestreit, S., Wang, N., Boivin, N.L., Douka, K., Richter, K.K., 2020a. Zooarchaeology by Mass Spectrometry (ZooMS) for Bone Material - Acid Insoluble Protocol, protocols.io. <https://doi.org/10.17504/protocols.io.bf43jqyn>.
- Brown, S., Hebestreit, S., Wang, N., Boivin, N.L., Douka, K., Richter, K.K., 2020b. Zooarchaeology by Mass Spectrometry (ZooMS) for Bone Material - Acid Soluble Protocol, protocols.io. <https://doi.org/10.17504/protocols.io.bf5bjq2n>.
- Brown, S., Douka, K., Collins, M.J., Richter, K.K., 2021a. On the standardization of ZooMS nomenclature. *J. Proteomics* 235, 104041. <https://doi.org/10.1016/j.jprot.2020.104041>.
- Brown, S., Wang, N., Oertle, A., Kozlikin, M.B., Shunkov, M.V., Derevianko, A.P., Comeskey, D., Jope-Street, B., Harvey, V.L., Chowdhury, M.P., Buckley, M., Higham, T., Douka, K., 2021b. Zooarchaeology through the lens of collagen fingerprinting at Denisova Cave. *Sci. Rep.* 11, 15457. <https://doi.org/10.1038/s41598-021-94731-2>.
- Buckley, M., Collins, M., Thomas-Oates, J., Wilson, J.C., 2009. Species identification by analysis of bone collagen using matrix-assisted laser desorption/ionisation time-of-flight mass spectrometry. *Rapid Commun. Mass Spectrom.* 23, 3843–3854. <https://doi.org/10.1002/rcm.4316>.
- Buckley, M., Gu, M., Shameer, S., Patel, S., Chamberlain, A.T., 2016. High-throughput collagen fingerprinting of intact microfaunal remains; a low-cost method for distinguishing between murine rodent bones. *Rapid Commun. Mass Spectrom.* 30, 805–812. <https://doi.org/10.1002/rcm.7483>.
- Buckley, M., Harvey, V.L., Chamberlain, A.T., 2017. Species identification and decay assessment of Late Pleistocene fragmentary vertebrate remains from Pin Hole Cave (Creswell Crags, UK) using collagen fingerprinting. *Boreas* 46, 402–411. <https://doi.org/10.1111/bor.12225>.
- Buckley, M., Gu, M., Herman, J., Junno, J.-A., Denys, C., Chamberlain, A.T., 2018. Species identification of voles and lemmings from late Pleistocene deposits in Pin Hole cave (Creswell Crags, UK) using collagen fingerprinting. *Quat. Int.* 483, 83–89. <https://doi.org/10.1016/j.quaint.2018.03.015>.
- Buckley, M., Herman, J., 2019. Species identification of Late Pleistocene bat bones using collagen fingerprinting. *Int. J. Osteoarchaeol.* 29, 1051–1059. <https://doi.org/10.1002/oa.2818>.
- Child, M.F., Monadjem, A., 2016a. *Dendromus melatonis*. The IUCN Red List of Threatened Species 2016: e.T6443A22235350. <https://doi.org/10.2305/IUCN.UK.2016-3RLTS.T6443A22235350.en>.
- Child, M.F., Monadjem, A., 2016b. *Dendromus mesomelas*. The IUCN Red List of Threatened Species 2016: e.T6444A22235226, 10.2305.IUCN.UK.2016-3.RLTS.T6444A22235226.en.
- Coutu, A.N., Whitelaw, G., Le Roux, P., Sealy, J., 2016. Earliest evidence for the ivory trade in southern Africa: isotopic and ZooMS analysis of seventh-tenth century AD ivory from KwaZulu-natal. *Afr. Archaeol. Rev.* 33, 411–435. <https://doi.org/10.1007/s10437-016-9232-0>.
- Coutu, A.N., Taurozzi, A.J., Mackie, M., Jensen, T.Z.T., Collins, M.J., Sealy, J., 2021. Palaeoproteomics confirm earliest domesticated sheep in southern Africa ca. 2000 BP. *Sci. Rep.* 11, 6631. <https://doi.org/10.1038/s41598-021-85756-8>.
- d'Errico, F., Banks, W.E., Warren, D.L., Sgubin, G., van Niekerk, K., Henshilwood, C., Daniau, A.-L., Sánchez Goñi, M.F., 2017. Identifying early modern human ecological niche expansions and associated cultural dynamics in the South African Middle Stone Age. *Proc. Natl. Acad. Sci. USA* 114, 7869–7876. <https://doi.org/10.1073/pnas.1620752114>.
- De Graaff, G., 1981. *The Rodents of South Africa*. Butterworths, Durban.
- Demarchi, B., Hall, S., Roncal-Herrero, T., Freeman, C.L., Woolley, J., Crisp, M.K., Wilson, J.C., Fotakis, A.K., Fischer, R., Kessler, B., Jersie-Christensen, R.R., Olsen, J. V., Haile, J., Thomas, J.A., Marean, C.W., Parkington, J., Presslee, S., Lee-Thorp, J., Ditchfield, P., Hamilton, J.F., Ward, M.W., Wang, C.M., Shaw, M.D., Harrison, T., Domínguez-Rodrigo, M., MacPhee, R.D.E., Kwekason, A., Ecker, M., Horwitz, L.K., Chazan, M., Kröger, R., Thomas-Oates, J., Harding, J.H., Cappellini, E., Penkman, K., Collins, M., 2016. Protein sequences bound to mineral surfaces persist into deep time. *Elife* 5, e17092. <https://doi.org/10.7554/eLife.17092>.
- Demarchi, B., Mackie, M., Li, Z., Deng, T., Collins, M.J., Clarke, J., 2022. Survival of mineral-bound peptides into the Miocene. *Elife* 11, e82849. <https://doi.org/10.7554/eLife.82849>.
- Glue, D.E., 1967. Prey taken by the barn owl in England and Wales. *Hous. Theor. Soc.* 14, 169–183.
- Harvey, V.L., Egerton, V.M., Chamberlain, A.T., Manning, P.L., Sellers, W.I., Buckley, M., 2019. Interpreting the historical terrestrial vertebrate biodiversity of cayman brack (greater antilles, caribbean) through collagen fingerprinting. *Holocene* 29, 531–542. <https://doi.org/10.1177/0959683618824793>.
- Heisler, L.M., Somers, C.M., Poulin, R.G., 2016. Owl pellets: a more effective alternative to conventional trapping for broad-scale studies of small mammal communities. *Methods Ecol. Evol.* 7, 96–103. <https://doi.org/10.1111/2041-210X.12454>.
- Henshilwood, C.S., van Niekerk, K.L., Wurz, S., Delagnes, A., Armitage, S.J., Rifkin, R.F., Douze, K., Keene, P., Haaland, M.M., Reynard, J., Discamps, E., Mienies, S.S., 2014.

- Klipdrift shelter, southern Cape, South Africa: preliminary report on the Howiesons Poort layers. *J. Archaeol. Sci.* 45, 284–303. <https://doi.org/10.1016/j.jas.2014.01.033>.
- IUCN. 2022. *The IUCN Red List of Threatened Species, 1 ed, p. 2022, Version*.
- Janzen, A., Richter, K.K., Mwebi, O., Brown, S., Onduso, V., Gatwiri, F., Ndiema, E., Katongo, M., Goldstein, S.T., Douka, K., Boivin, N., 2021. Distinguishing african bovids using zooarchaeology by mass spectrometry (ZooMS): new peptide markers and insights into iron age economies in Zambia. *PLoS One* 16, e0251061. <https://doi.org/10.1371/journal.pone.0251061>.
- Jensen, T.Z.T., Sjöström, A., Fischer, A., Rosengren, E., Lanigan, L.T., Bennike, O., Richter, K.K., Gron, K.J., Mackie, M., Mortensen, M.F., Sørensen, L., Chivall, D., Iversen, K.H., Tauruzzi, A.J., Olsen, J., Schroeder, H., Milner, N., Sørensen, M., Collins, M.J., 2020. An integrated analysis of Maglemose bone points reframes the Early Mesolithic of Southern Scandinavia. *Sci. Rep.* 10, 17244 <https://doi.org/10.1038/s41598-020-74258-8>.
- Kontopoulos, I., Penkman, K., Mullin, V.E., Winkelbach, L., Unterländer, M., Scheu, A., Kreutzer, S., Hansen, H.B., Margaryan, A., Teasdale, M.D., Gehlen, B., Street, M., Lynnerup, N., Liritzis, I., Sampson, A., Papageorgopoulou, C., Allentoft, M.E., Burger, A.O., Bradley, D.G., Collins, P., Katongo, M., Kwekason, A., Laird, M.F., Lewis, J., Mabulla, A.Z.P., Mampemba, F., Morris, A., Mudenda, G., Mwafurirwa, R., Mwangomba, D., Ndiema, E., Ogola, C., Schilt, F., Willoughby, P.R., Wright, D.K., Zipkin, A., Pinhasi, R., Kennett, D.J., Manthi, F.K., Rohland, N., Patterson, N., Reich, D., Prendergast, M.E., 2022. Ancient DNA and deep population structure in sub-Saharan African foragers. *Nature* 603, 290–296. <https://doi.org/10.1038/s41586-022-04430-9>.
- Lugli, F., Sciotto, G., Oliveri, P., Malegori, C., Prati, S., Gatti, L., Silverstrini, S., Romandini, M., Catelli, E., Casale, M., Talamo, S., Iacumin, P., Benazzi, S., Mazzeo, R., 2021. Near-infrared hyperspectral imaging (NIR-HSI) and normalized difference image (NDI) data processing: an advanced method to map collagen in archaeological bones. *Talanta* 226, 122126. <https://doi.org/10.1016/j.talanta.2021.122126>.
- Mackay, A., Stewart, B.A., Chase, B.M., 2014. Coalescence and fragmentation in the late Pleistocene archaeology of southernmost Africa. *J. Hum. Evol.* 72, 26–51. <https://doi.org/10.1016/j.jhevol.2014.03.003>.
- Mackay, A., Armitage, S.J., Niespolo, E.M., Sharp, W.D., Stahlschmidt, M.C., Blackwood, A.F., Boyd, K.C., Chase, B.M., Lagle, S.E., Kaplan, C.F., Low, M.A., Martisusi, N.L., McNeill, P.J., Moffat, I., O'Driscoll, C.A., Rudd, R., Orton, J., Steele, T.E., 2022. Environmental influences on human innovation and behavioural diversity in southern Africa 92–80 thousand years ago. *Nature Ecology & Evolution* 6, 361–369. <https://doi.org/10.1038/s41559-022-01667-5>.
- Marean, C.W., Cowling, R.M., Franklin, J., 2020. The palaeo-agulhas plain: temporal and spatial variation in an extraordinary extinct ecosystem of the Pleistocene of the Cape floristic region. *Quat. Sci. Rev.* 235, 106161 <https://doi.org/10.1016/j.quascirev.2019.106161>.
- Matthews, T., 2004. *The Taphonomy and Taxonomy of Mio-Pliocene and Late Middle Pleistocene Micromammals from the Cape West Coast, South Africa*. University of Cape Town, South Africa, Cape Town.
- Matthews, T., Denys, C., Parkinson, J.E., 2005. The palaeoecology of the micromammals from the late middle Pleistocene site of Hoedjiespunt 1 (Cape Province, South Africa). *J. Hum. Evol.* 49, 432–451. <https://doi.org/10.1016/j.jhevol.2005.05.006>.
- Matthews, T., Marean, C., Nilssen, P., 2009. Micromammals from the middle Stone age (92–167 ka) at cave PP13B, Pinnacle point, south coast, South Africa. *Palaeontol. Afr.* 44, 112–120.
- Matthews, T., Rector, A., Jacobs, Z., Herries, A.I.R., Marean, C.W., 2011. Environmental implications of micromammals accumulated close to the MIS 6 to MIS 5 transition at Pinnacle point cave 9 (mossel Bay, western Cape Province, South Africa). *Palaeogeogr. Palaeoclimatol. Palaeoecol.* 302, 213–229.
- Matthews, T., Marean, C.W., Cleghorn, N., 2020. Past and present distributions and community evolution of Muridae and Soricidae from MIS 9 to MIS 1 on the edge of the Palaeo-Agulhas Plain (south coast, South Africa). *Quat. Sci. Rev.* 235, 105774 <https://doi.org/10.1016/j.quascirev.2019.05.026>.
- Matthews, T., Nel, T.H., 2021. The cryptic case of *Otomys sloggetti* (Sloggett's vlei rat): interpreting murid molar morphology in the fossil record. *South Afr. J. Sci.* 117 <https://doi.org/10.17159/sajs.2021/7137>, [10.1016/j.palaeo.2011.01.014](https://doi.org/10.1016/j.palaeo.2011.01.014).
- McBrearty, S., Brooks, A.S., 2000. The revolution that wasn't: a new interpretation of the origin of modern human behavior. *J. Hum. Evol.* 39, 453–563. <https://doi.org/10.1006/jhev.2000.0435>.
- Monadjem, A., Taylor, P.J., Denys, C., Cotterill, F.P.D., 2015. *Rodents of Sub-saharan Africa: A Biogeographic and Taxonomic Synthesis*. Walter de Gruyter, Berlin.
- Nel, T.H., 2013. *Micromammals, Climate Change and Human Behaviour in the Middle Stone Age, Southern Cape, South Africa - Examining the Possible Links between Palaeoenvironments and the Cognitive Evolution of Homo sapiens*. University of Bergen, Bergen.
- Nel, T.H., Henshilwood, C.S., 2016. The small mammal sequence from the c. 76 – 72 ka still Bay levels at Blombos cave, South Africa – taphonomic and palaeoecological implications for human behaviour. *PLoS One* 11, e0159817. <https://doi.org/10.1371/journal.pone.0159817>.
- Nel, T.H., Wurz, S., Henshilwood, C.S., 2018. Small mammals from marine isotope stage 5 at Klasies River, South Africa—reconstructing the local palaeoenvironment. *Quat. Int.* 471, 6–20. <https://doi.org/10.1016/j.quaint.2017.08.074>.
- Nel, T.H., Henshilwood, C.S., 2021. The 100,000–77,000-year old middle Stone age micromammal sequence from Blombos cave, South Africa: local climatic stability or a tale of predator bias? *Afr. Archaeol. Rev.* 38, 443–476. <https://doi.org/10.1007/s10437-021-09444-8>.
- Peters, C., Richter, K.K., Manne, T., Dortch, J., Paterson, A., Travouillon, K., Louys, J., Price, G.J., Petraglia, M., Crowther, A., Boivin, N., 2021. Species Identification of Australian Marsupials Using Collagen Fingerprinting, vol. 8. Royal Society Open Science, 211229. <https://doi.org/10.1098/rsos.211229>.
- Pothier Bouchard, G., Mentzer, S.M., Riel-Salvatore, J., Hodgkins, J., Miller, C.E., Negrino, F., Wogelius, R., Buckley, M., 2019. Portable FTIR for on-site screening of archaeological bone intended for ZooMS collagen fingerprint analysis. *J. Archaeol. Sci.: Report* 26, 101862. <https://doi.org/10.1016/j.jasrep.2019.05.027>.
- Prendergast, M.E., Buckley, M., Crowther, A., Frantz, L., Eager, H., Lebrasseur, O., Hutterer, R., Hulme-Beaman, A., Van Neer, W., Douka, K., Veall, M.-A., Morales, E. M.Q., Schuenemann, V.J., Reiter, E., Allen, R., Dimopoulos, E.A., Helm, R.M., Shipton, C., Mwebi, O., Denys, C., Horton, M., Wynne-Jones, S., Fleisher, J., Radimilahy, C., Wright, H., Searle, J.B., Krause, J., Larson, G., Boivin, N.L., 2017. Reconstructing Asian faunal introductions to eastern Africa from multi-proxy biomolecular and archaeological datasets. *PLoS One* 12, e0182565. <https://doi.org/10.1371/journal.pone.0182565>.
- Reed, D., Dirks, W., McMaster, L., Harrison, T., 2019. Accuracy of environmental reconstruction based on a blind test of micromammal evidence from East Africa. *Hist. Biol.* 31, 243–252. <https://doi.org/10.1080/08912963.2017.1360295>.
- Reynard, J.P., Discamps, E., Badenhorst, S., van Niekerk, K., Henshilwood, C.S., 2016a. Subsistence strategies in the southern Cape during the Howiesons Poort: taphonomic and zooarchaeological analyses of Klipdrift shelter, South Africa. *Quat. Int.* 404, 2–19. <https://doi.org/10.1016/j.quaint.2015.07.041>.
- Reynard, J.P., Discamps, E., Wurz, S., van Niekerk, K.L., Badenhorst, S., Henshilwood, C. S., 2016b. Occupational intensity and environmental changes during the Howiesons Poort at Klipdrift shelter, southern Cape, South Africa. *Palaeogeogr. Palaeoclimatol. Palaeoecol.* 449, 349–364. <https://doi.org/10.1016/j.palaeo.2016.02.035>.
- Richter, K.K., McGrath, K., Masson-MacLean, E., Hickinbotham, S., Tedder, A., Britton, K., Bottomley, Z., Dobney, K., Hulme-Beaman, A., Zona, M., Fischer, R., Collins, M., Speller, C., 2020. What's the catch? Archaeological application of rapid collagen-based species identification. *J. Archaeol. Sci.* 116, 105116 <https://doi.org/10.1016/j.jas.2020.105116>.
- Roberts, P., Henshilwood, C.S., van Niekerk, K.L., Keene, P., Gledhill, A., Reynard, J., Badenhorst, S., Lee-Thorp, J., 2016. Climate, environment and early human innovation: stable isotope and faunal proxy evidence from archaeological sites (98–59ka) in the southern Cape, South Africa. *PLoS One* 11, e0157408. <https://doi.org/10.1371/journal.pone.0157408>.
- Ruebens, K., Smith, G.M., Fewlass, H., Sinet-Mathiot, V., Hublin, J.-J., Welker, F., 2023. Neanderthal subsistence, taphonomy and chronology at Salzgitter-Lebenstedt (Germany): a multifaceted analysis of morphologically unidentifiable bone. *Journal of Quaternary Science n/a*. <https://doi.org/10.1002/jqs.3499>.
- Silverstrini, S., Lugli, F., Romandini, M., Real, C., Sommella, E., Salviati, E., Arrighi, S., Bortolini, E., Figus, C., Higgins, O.A., Marciangi, G., Oxilia, G., Delpiano, D., Vazzana, A., Piperno, M., Crescenzi, C., Campiglia, P., Collina, C., Peresani, M., Spinapolic, E.E., Benazzi, S., 2022. Integrating ZooMS and zooarchaeology: new data from the Uluzzian levels of Uluzzo C Rock Shelter, Rocca San Sebastiano cave and Riparo del Broion. *PLoS One* 17, e0275614. <https://doi.org/10.1371/journal.pone.0275614>.
- Sinet-Mathiot, V., Smith, G.M., Romandini, M., Wilcke, A., Peresani, M., Hublin, J.-J., Welker, F., 2019. Combining ZooMS and zooarchaeology to study late Pleistocene hominin behaviour at fumane (Italy). *Sci. Rep.* 9, 12350 <https://doi.org/10.1038/s41598-019-48706-z>.
- Skinner, J.D., Chimimba, C.T., 2005. *The Mammals of the Southern African Sub-region*. Cambridge University Press, Cambridge.
- Sponheimer, M., Ryder, C.M., Fewlass, H., Smith, E.K., Pestle, W.J., Talamo, S., 2019. Saving Old Bones: a non-destructive method for bone collagen prescreening. *Sci. Rep.* 9, 13928 <https://doi.org/10.1038/s41598-019-50443-2>.
- Stoetzel, E., Marion, L., Nespoulet, R., El Hajraoui, M.A., Denys, C., 2011. Taphonomy and palaeoecology of the late Pleistocene to middle Holocene small mammal succession of El Harhoura 2 cave (Rabat-Témara, Morocco). *J. Hum. Evol.* 60, 1–33. <https://doi.org/10.1016/j.jhevol.2010.07.016>.
- Stoetzel, E., Sime, W.B., Pleurdeau, D., Asrat, A., Assefa, Z., Desclaux, E., Denys, C., 2018. Preliminary study of the rodent assemblages of Goda Buticha: new insights on Late Quaternary environmental and cultural changes in southeastern Ethiopia. *Quat. Int.* 471, 21–34. <https://doi.org/10.1016/j.quaint.2017.08.050>.
- Van der Sluis, L.G., Hollund, H.L., Buckley, M., De Louw, P.G.B., Rijdsdijk, K.F., Kars, H., 2014. Combining histology, stable isotope analysis and ZooMS collagen fingerprinting to investigate the taphonomic history and dietary behaviour of extinct giant tortoises from the Mare aux Songes deposit on Mauritius. *Palaeogeogr. Palaeoclimatol. Palaeoecol.* 416, 80–91. <https://doi.org/10.1016/j.palaeo.2014.06.003>.
- Wang, N., Brown, S., Richter, K.K., Ditchfield, P., Hebestreit, S., Kozilikin, M., Luu, S., Wedage, O., Grimaldi, S., Chazen, M., Horwitz, L.K., Spriggs, M., Summerhayes, G., Shunkov, M., Douka, K., 2021. Testing the efficacy and comparability of ZooMS protocols on archaeological bone. *J. Proteomics* 233, 104078, [10.1016/j.jprot.2020.104078](https://doi.org/10.1016/j.jprot.2020.104078).

- Welker, F., Soressi, M., Rendu, W., Hublin, J.-J., Collins, M., 2015. Using ZooMS to identify fragmentary bone from the late middle/early upper palaeolithic sequence of les cottés, France. *J. Archaeol. Sci.* 54, 279–286. <https://doi.org/10.1016/j.jas.2014.12.010>.
- Welker, F., Hajdinjak, M., Talamo, S., Jaouen, K., Dannemann, M., David, F., Julien, M., Meyer, M., Kelso, J., Barnes, I., Brace, S., Kamminga, P., Fischer, R., Kessler, B., Stewart, J.R.M., Pääbo, S., Collins, M., Hublin, J.-J., 2016. Palaeoproteomic evidence identifies archaic hominins associated with the Châtelperronian at the Grotte du Renne. *Proc. Natl. Acad. Sci. USA* 113, 11162–11167. <https://doi.org/10.1073/pnas.1605834113>.
- Welker, F., Soressi, M.A., Roussel, M., van Riemsdijk, I., Hublin, J.-J., Collins, M.J., 2017. Variations in glutamine deamidation for a Châtelperronian bone assemblage as measured by peptide mass fingerprinting of collagen. *Star: Science & Technology of Archaeological Research* 3, 15–27. <https://doi.org/10.1080/20548923.2016.1258825>.
- Welker, F., Ramos-Madrigal, J., Kuhlwil, M., Liao, W., Gutenbrunner, P., de Manuel, M., Samodova, D., Mackie, M., Allentoft, M.E., Bacon, A.-M., Collins, M.J., Cox, J., Lalueza-Fox, C., Olsen, J.V., Demeter, F., Wang, W., Marques-Bonet, T., Cappellini, E., 2019. Enamel proteome shows that *Gigantopithecus* was an early diverging pongine. *Nature* 576, 262–265. <https://doi.org/10.1038/s41586-019-1728-8>.